



High temperature oxidation of iron-based alloys reinforced by hafnium carbides. Part 2: Metallography results

Patrice Berthod*, Elodie Conrath

Institut Jean Lamour (UMR 7198), Team 206 "Surface and Interface, Chemical Reactivity of Materials", University of Lorraine, Faculty of Sciences and Technologies, B.P. 70239, 54506 Vandoeuvre-lès-Nancy, (FRANCE)

E-mail : Patrice.Berthod@univ-lorraine.fr

ABSTRACT

The behaviour in oxidation at 1200°C of three HfC-containing iron-based alloys – Fe - 25Cr - 0.25 or 0.50C - 3.72 or 5.58Hf (wt.%) – was studied at 1200°C in dry synthetic air. After a first part dealing with the mass variations recorded by thermogravimetry during the oxidation tests, the present second part aims to characterize the surface, subsurface and bulk deteriorations or modifications by observing (optical and electron microscopy) and analysing (EDS, XRD) the oxidized samples before and after cross-sectioning. The results show that no catastrophic oxidation occurred neither for the Hf-containing alloys nor for the corresponding Hf-free ones added for comparison. However iron oxides were present together with chromia in the external scale – with additionally some hafnium oxides – and internal oxidation seemingly occurred deeply. Despite that the chromium contents in extreme surface were still high oxidation acceleration starts were observed in some isolated areas. The oxidation behaviour of these iron-based Hf-containing alloys was globally much better than for their cobalt-based homologues and slightly worse than for their nickel-based ones. © 2014 Trade Science Inc. - INDIA

KEYWORDS

Iron-based alloys;
Hafnium carbides;
High temperature oxidation;
Post-mortem
characterization.

INTRODUCTION

Iron is one of the most interesting elements as base element for high temperature metallic alloy, by considering its high value of {fusion's point / cost} ratio. Indeed, presenting a melting point as high as 1535°C^[1] and being significantly cheaper than its neighbours in the Mendeleiev's table (notably nickel and cobalt), Fe is often used in superalloys for constituting their matrix, but the most often in association with nickel to favour the solidification as austenitic dendrites and to keep this

FCC compact crystalline network at lower temperatures^[2,3]. The nickel addition slightly improves the behaviour of iron-based alloys in oxidation at high temperature but chromium is essential to allow such iron-based alloys to resist hot corrosion^[4]. Besides the well-known austenitic stainless steels^[5] – iron-based alloys simultaneously rich in nickel and chromium (e.g. 10wt.%Ni and 18wt.% Cr) – which can be used at temperature rather medium than really high, highly refractory iron alloys can be obtained with 30wt.% of chromium and tantalum carbides interdendritically dis-

persed^[6,7]. Such carbides can be effectively obtained by adding tantalum and carbon in similar quantities in the chemical composition to obtain eutectic {script-like}-shaped TaC carbides insuring mutual dendrites fixing and then higher mechanical resistance at high temperature^[7]. To achieve such high mechanical potential in hot conditions other {high temperature}-stable carbides can be considered, as hafnium carbides. To obtain HfC carbides with a density high enough rather high contents in hafnium must be present (with the corresponding quantity in carbon)^[8]. One logically thinks that this may greatly influence the behaviour of the alloys in high temperature oxidation by taking into account the reactive character of this element.

To better know how fast HfC-containing iron-based alloys oxidize at high temperature thermogravimetry tests were carried out at 1200°C for 46 hours in industrial air. The kinetic results, previously presented in the first part of this work^[9], showed that mass gains were speedier than the corresponding Hf-free iron alloys with the same chromium and carbon contents, with a particular fast oxidation for the Hf-richest alloy. The aim of this second part is to examine the oxidized samples to understand the differences of behaviour due to the presence of hafnium in these iron-based alloys.

EXPERIMENTAL DETAILS

Elaboration of the alloys, thermogravimetry samples' preparation and oxidation tests

First it can be useful to remember that five iron-based alloys were tested in oxidation with mass gain recording. Their names (or targeted compositions) and the obtained chemical compositions are the following ones:

- “Fe-25Cr-0.25C-3.72Hf”: 25.71wt.% Cr and 3.87wt.%Hf (Co: bal., C: not measured)
- “Fe-25Cr-0.50C-3.72Hf”: 25.59wt.% Cr and 3.46wt.%Hf (Co: bal., C: not measured)
- “Fe-25Cr-0.50C-5.58Hf”: 27.23wt.% Cr and 4.85wt.%Hf (Co: bal., C: not measured)
- “Fe-25Cr-0.25C”: 25.47wt.% Cr (Co: bal., C: not measured)
- “Fe-25Cr-0.50C”: 24.52wt.% Cr (Co: bal., C: not measured)

They were all elaborated from pure elements by

high frequency induction melting in inert atmosphere and rather quickly solidified (rather low alloy quantity (40g) and water-cooled metallic mould). Parallelepipedic samples (about $10 \times 10 \times 3 \text{ mm}^3$) were obtained by cutting using precision saw, polished all around using 1200-grit SiC papers, and tested in a thermo-balance (Setaram TG92) according to the following thermal cycle: heating at +20K/min, isothermal stage at 1200°C for 46 hours, cooling at -5K/min.

Metallographic samples' preparation and characterization

After cooling to room temperature the oxidized samples were carefully extracted from the alumina-gained platinum “spider”, scanned using an office scanner, and analysed by X-ray Diffraction (Philips X'Pert Pro) for a first identification of the external oxides formed. Thereafter the samples were subjected to gold deposition using cathodic evaporation and electrolytic deposition of nickel to strengthen the external oxides before cutting. The nickel-covered samples were cut using a precision saw (Buelher Isomet 5000), embedded in a resin & hardener mixture (Escil) and polished until obtaining a mirror-like surface state (SiC papers from 240-grit to 1200-grit, ultrasonic washing and finished with textile disk enriched with 1 µm-alumina spray).

The mounted and polished samples were first observed using an optical microscope (Olympus BX51) equipped with a digital camera driven by the DP-Soft software of Olympus. Optical micrographs were taken on the external oxides visible in cross-sections, the analyses of which were performed using the EDS apparatus of a Scanning Electron Microscope (SEM) JEOL J7600F to complete their identification. The bulk microstructures were examined using another SEM (JEOL JSM6010LA), in Back Scattered Electrons Mode (BSE).

RESULTS AND DISCUSSION

Initial microstructures of the alloys

One can remind that the two ternary Fe-25Cr-0.25 and 0.50C alloys initially contained chromium carbides while the three Hf-containing alloys contained interdendritic HfC carbides, exclusively or additionally (Figure 0). The 0.25wt.%C-containing alloy presented

Full Paper

only HfC carbides (the white ones in BSE mode) while the two 0.50wt.%C-containing ones also contain chromium carbides (the dark ones).

chromia and Fe_2O_3 but no mixed oxide was detected. Another difference with the oxidized Hf-free alloys is the existence of hafnium oxide (HfO_2) the presence of

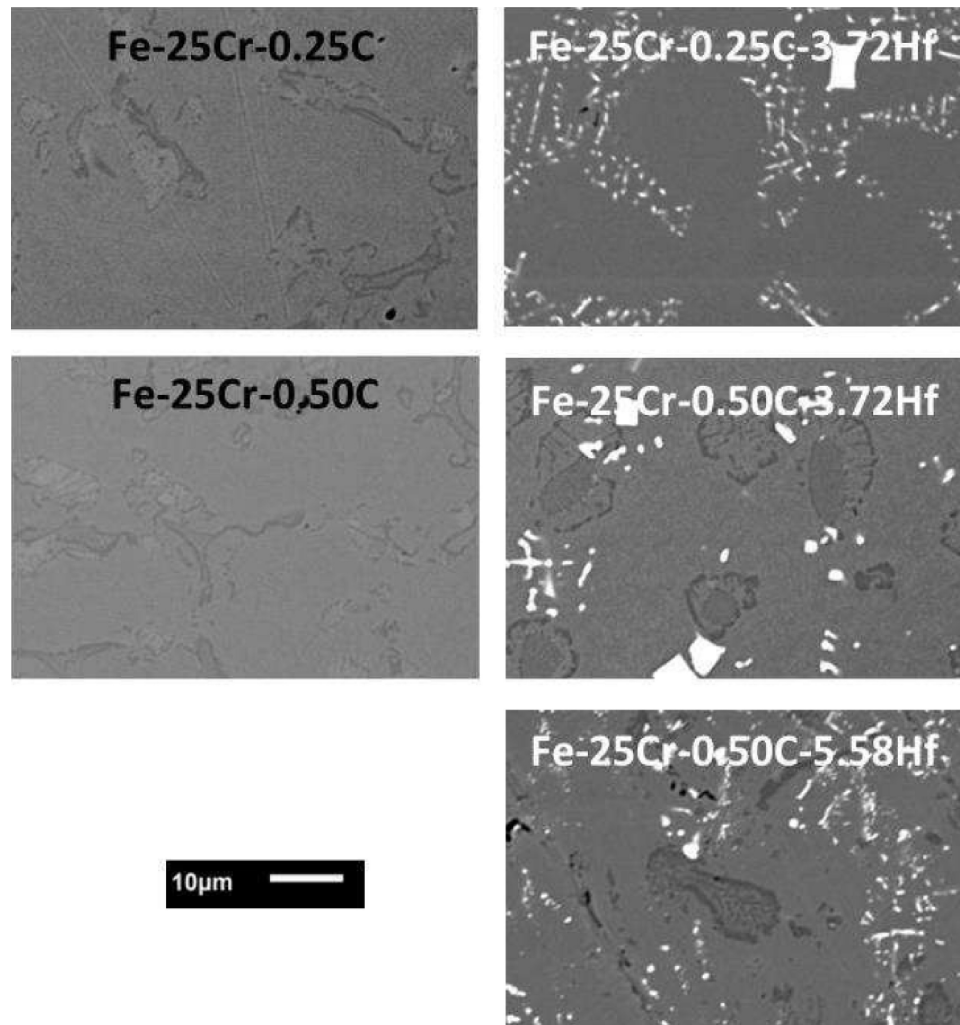


Figure 0 : Remembering the as-cast microstructures of the two Hf-free alloys (left) and of the three HfC-containing alloys (right)

Surface characterization of the oxides

Before being metallographically characterized the oxidized samples were scanned. The obtained pictures (for one face out of two) are presented in Figure 1. One can see that the external oxide was partly lost in the cases of the Fe-0.50C-3.72Hf alloy and of the Fe-25Cr-0.25C alloy, which well corresponds to the differences seen -- in the first part of this work^[9] (dealing with the thermogravimetry measurements) -- between the mass gain achieved during the isothermal stage and the final mass gain after return to room temperature.

The aspect of the oxidized samples is rather rugged, this letting thinking that oxidation led here and there

to specific oxides in addition to the uniform scales. X-ray diffraction runs were performed on the oxidized surfaces of all these samples and it appeared that several oxides were effectively present, as illustrated by the two XRD diffractograms corresponding to the Hf-free 0.25C-containing alloy (Figure 2) and the Hf-containing alloy with the same amount in carbon (Figure 3).

One can see that not only chromia (Cr_2O_3) is present in the oxide scale developed around the 0.25C-containing ternary alloy but that there are also Fe_2O_3 and a mixed oxide $(\text{Fe,Cr})_2\text{O}_3$. The same features were obtained for the Hf-free 0.50C-containing alloy.

The three Hf-containing alloys were all covered with

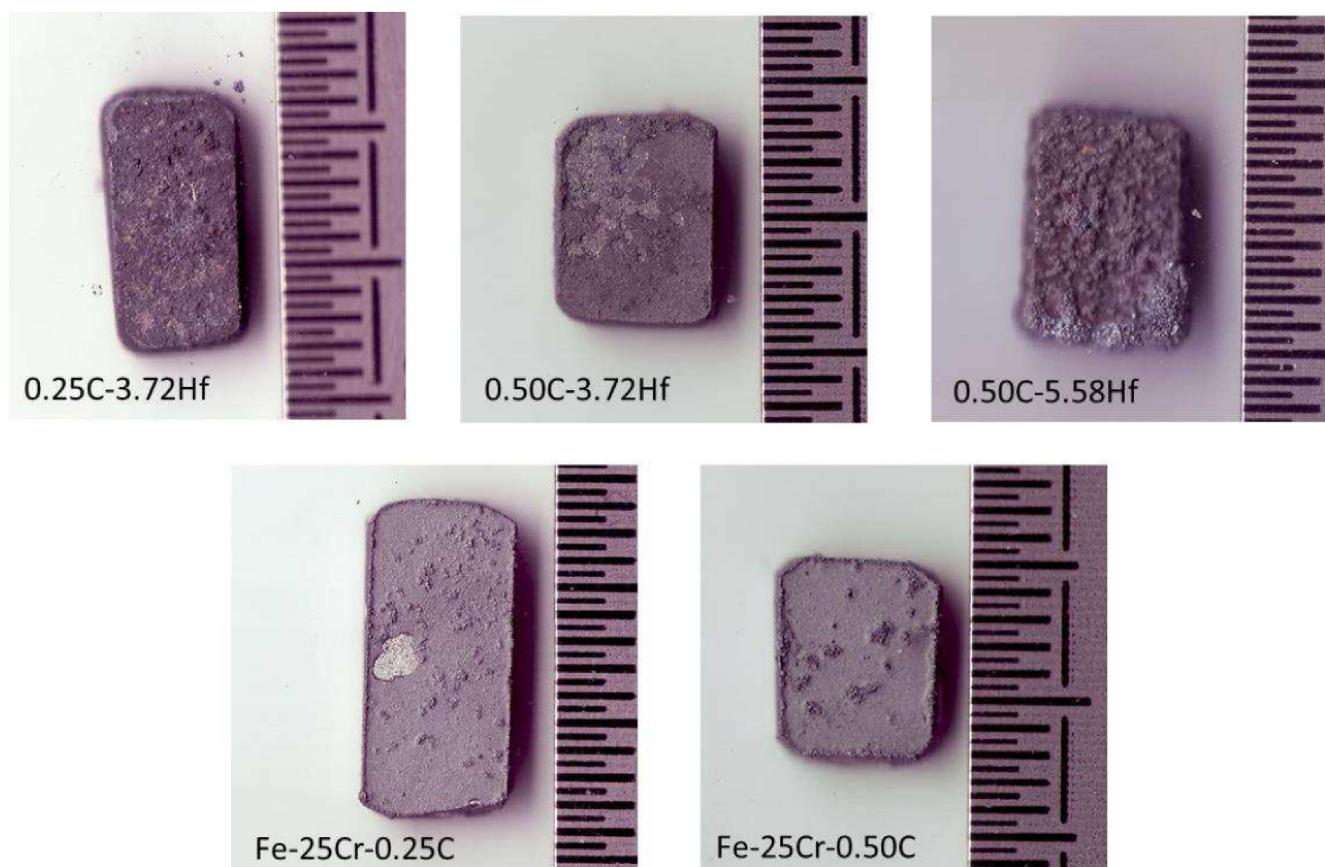


Figure 1 : External aspects of the oxidized samples when observed before metallographic preparation

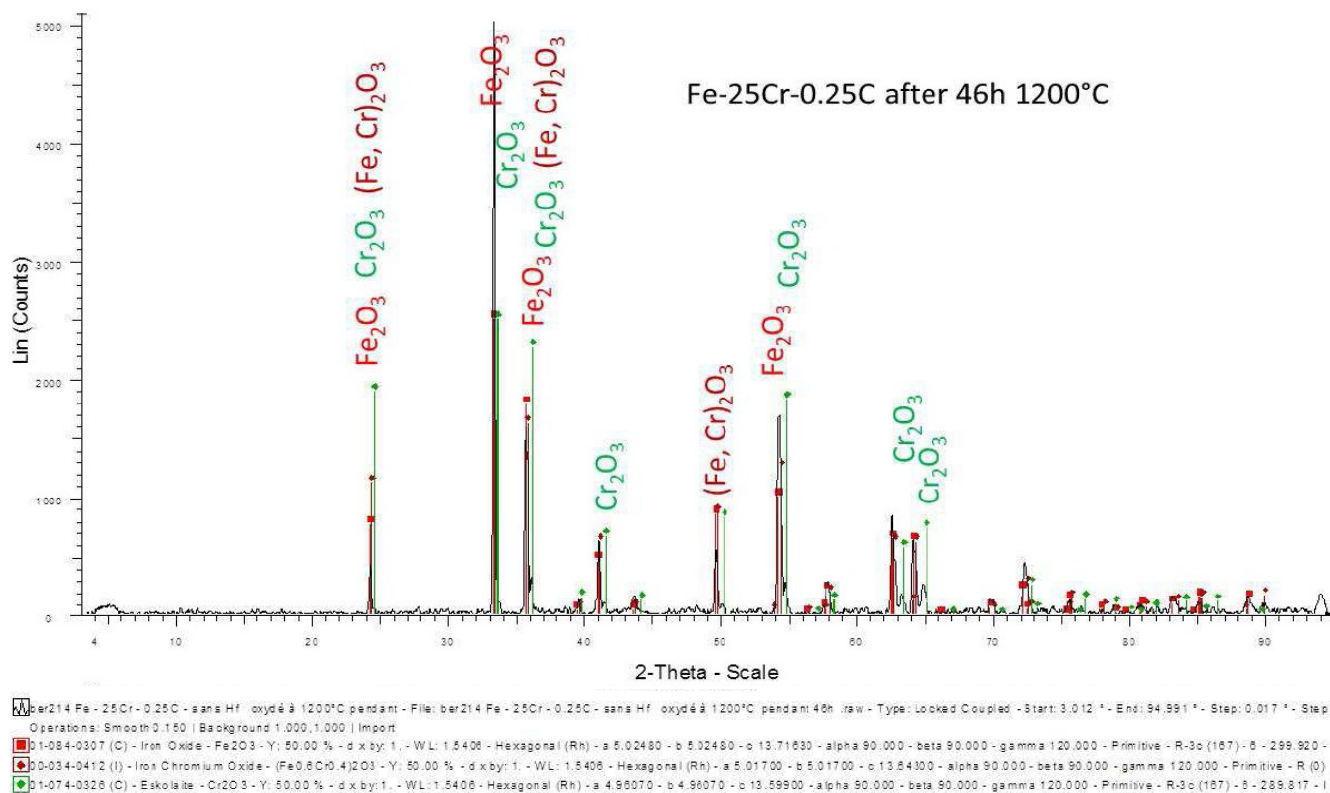


Figure 2 : Diffractogram acquired on the oxidized surface of the Hf-free 0.25C-containing alloy

Full Paper

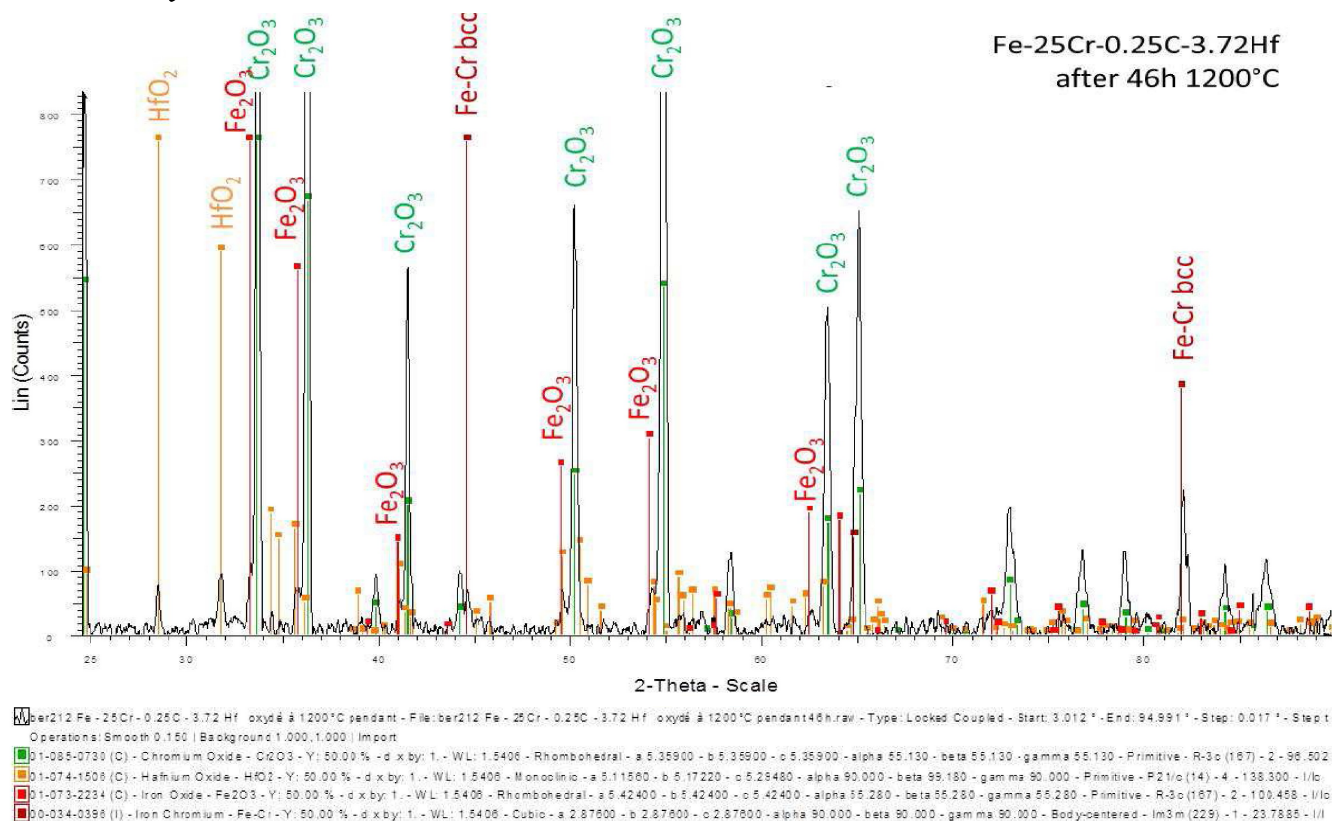


Figure 3 : Diffractogram acquired on the oxidized surface of the (Hf, 0.25C)-containing alloy

which was clearly evidenced by XRD since rather high peaks corresponding to this oxide were obtained in the XRD diffractograms acquired for the three alloys containing Hf.

Characterization of the oxides in cross-section

After classical metallographic preparation the five oxidized samples were examined in cross-section, by optical microscopy. Several optical micrographs were taken and some of them are displayed in Figure 3 (Hf-free alloys) and in Figure 4 (Hf-containing alloys) for illustrating the surface and subsurface states.

One can see on these micrographs (two magnifications) that there are obviously often at least two types of oxides present (different gray levels), as previously demonstrated by the XRD results (Figure 2 and Figure 3). In addition there are here and there particularly thick oxides zone, with a part penetrating in the alloy and another part being in relief by regards to the surface of the external scale, confirming the roughness seen above on the pictures obtained by scanning (Figure 1).

The thickness of the external scale was measured on the optical micrographs and the results are graphi-

cally displayed in Figure 6. One can see that the continuous scale is of about the same thickness for all the alloys, containing Hf or not. In contrast, the discrete presence of additional oxides in some locations leads to much higher thicknesses, especially in the cases of the {0.25C-3.72Hf}- and {0.50C-5.58Hf}-containing alloys.

On the optical micrographs presented in Figure 5 one can also see that internal oxidation occurred in the Hf-containing alloys. The depth of internal oxidation, which is of about 45 μ m for the two Hf-free alloys, is significantly higher (about 250 μ m) for the two 3.72Hf-containing alloys in which the HfC carbides seem having been oxidized on place into HfO₂ (more visible than the initial carbides with optical microscopy). The 5.58Hf-containing alloy is internally oxidized in its whole thickness.

Some EDS pinpoint measurements were realized in the subsurface close to the oxide-alloy interface for the three Hf-containing alloys. This showed that the chromium content has logically decreased but it remained at a rather high level (around 20wt.% Cr against about 25wt.% initially).

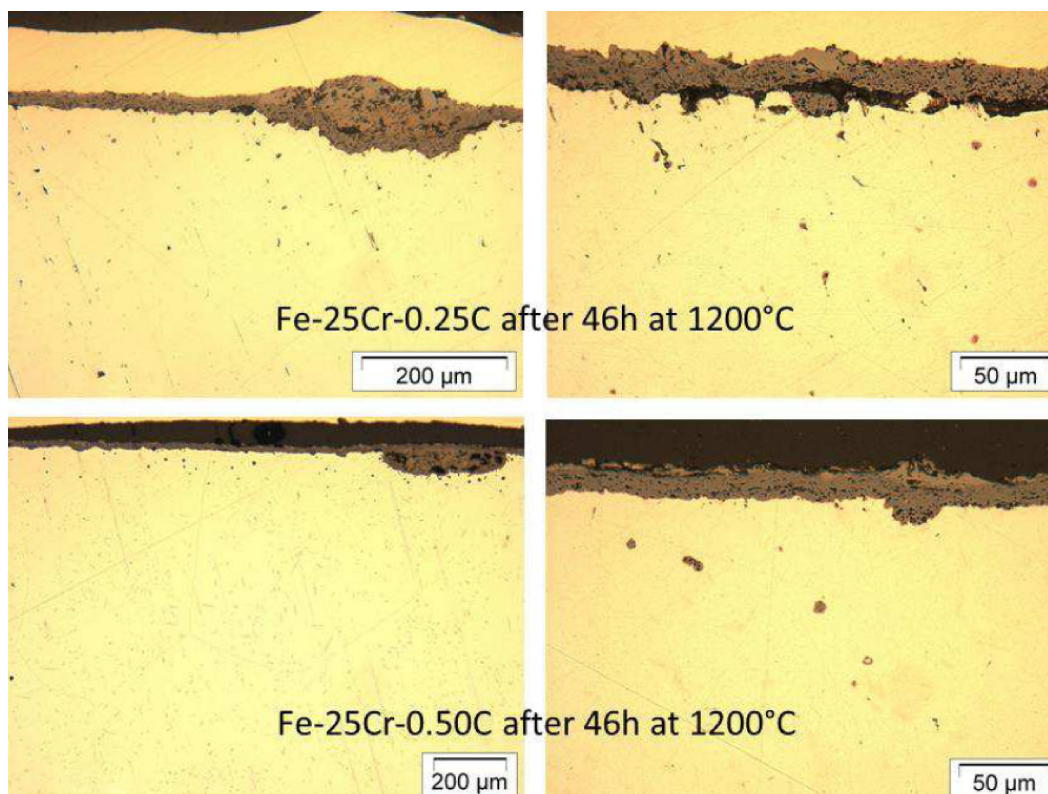


Figure 4 : The oxidized Hf-free alloys observed in cross-section (optical micrographs)

Bulk microstructure observations

It is also interesting to observe how behaved the microstructures of these alloys in the bulk of the samples during the oxidation tests which meant for them simply exposures at high temperature. These microstructures are illustrated by SEM/BSE micrographs in Figure 7 (Fe-25Cr-0.25C-3.72Hf), Figure 8 (Fe-25Cr-0.50C-3.72Hf) and Figure 9 (Fe-25Cr-0.50C-5.58Hf). In each case the initial microstructure is inserted in the corner top-right to allow comparison.

During the 46 hours spent at 1200°C the HfC carbides did not evolve in the Fe-25Cr-0.25C-3.72Hf (Figure 7) but more or less dark particles (that are probably chromium carbides) appeared. It was unfortunately not possible to specify these particles but one can wonder whether the darkest ones are Cr_7C_3 and the less dark ones Cr_{23}C_6 .

The same comments can be done concerning the Fe-25Cr-0.50C-3.72Hf alloy (Figure 8) and the Fe-25Cr-0.50C-5.58Hf alloy (Figure 9), despite it already contained chromium carbides in their as-cast condition.

General commentaries

As suggested in the first part of this work^[9] by the

thermogravimetry results, the oxidation of the three Hf-containing alloys was not catastrophic. If a chromia layer was often observed oxides of iron, or of chromium and iron together, were also present, with additionally hafnium oxide but these latter ones in much lower quantities. However, with mass gain kinetics remaining similar to the ones obtained for the nickel-based alloys with the same contents in Cr, C and Hf (except for 5.58wt.%Hf)^[10] (and much faster than the corresponding Hf-containing cobalt-based alloys)^[11], the more diversified compositions of the oxide scales of these Fe-based alloys rich in hafnium did not really threaten the rather good behaviour of these alloys. This is confirmed by the subsurface chromium contents remained rather high in extreme surface. However starts of locally faster oxidation were also observed here and there, microscopically as well as macroscopically and it is not sure that the relative good behaviour will continue for a long time.

The bulk microstructure – notably the carbides surface fractions and shapes – was obviously not really affected and one can guess that the mechanical properties will be kept at the same level all along the high temperature exposures. But one must be sure first that

Full Paper

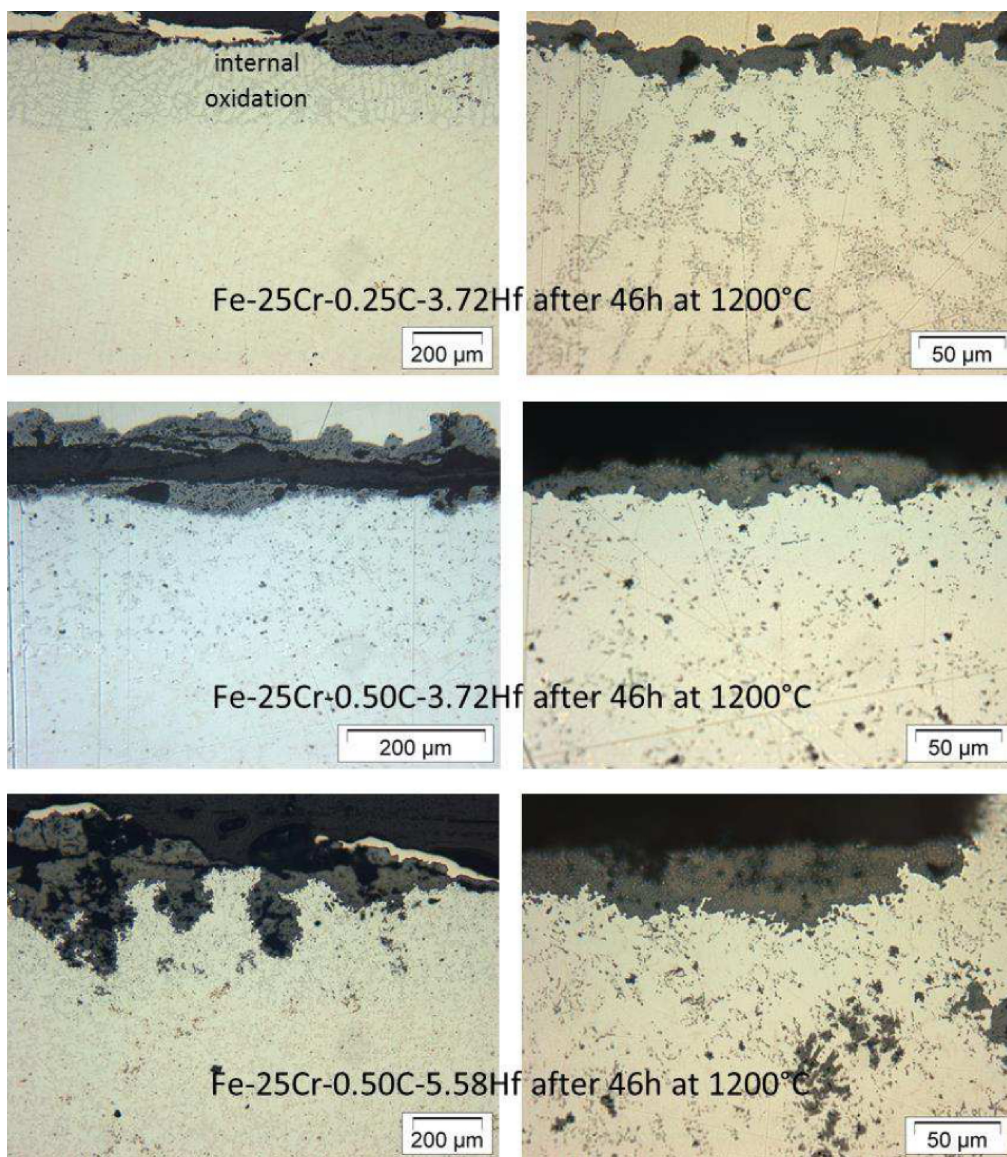


Figure 5 : The oxidized Hf-containing alloys observed in cross-section (optical micrographs)

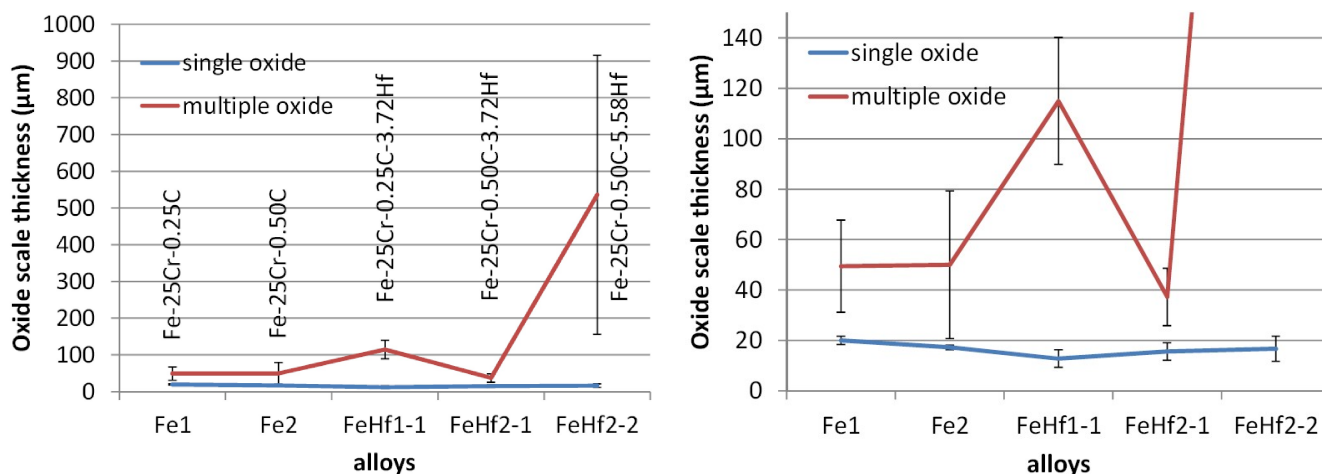


Figure 6 : Average and standard deviation of the thickness of the external scale measured on optical micrographs (left: full scale graph; right: enlargement of the same graph)

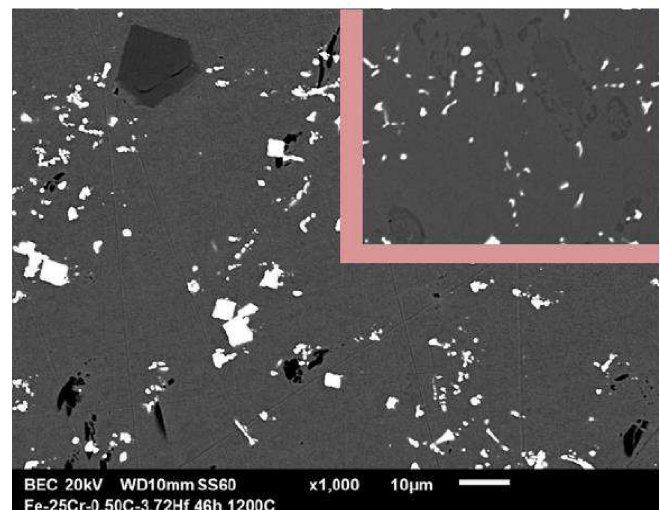
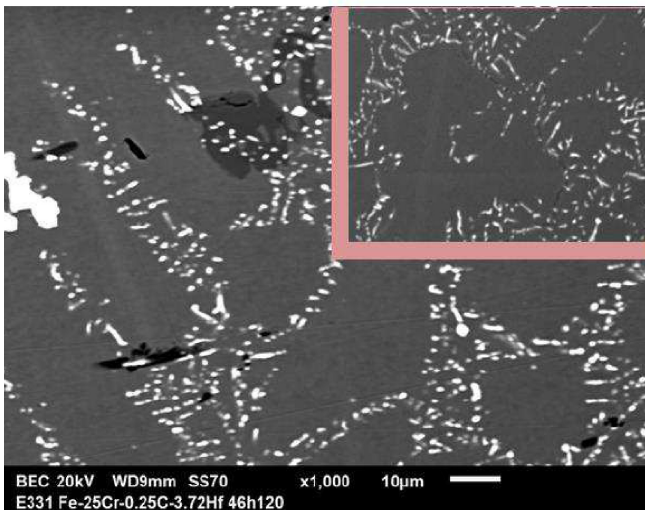
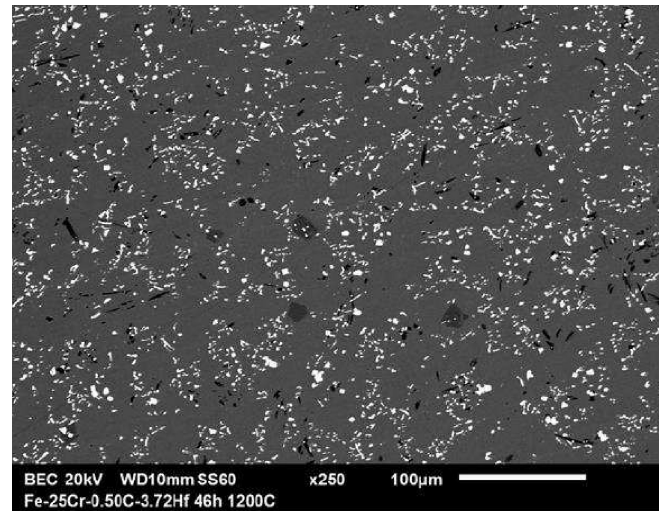
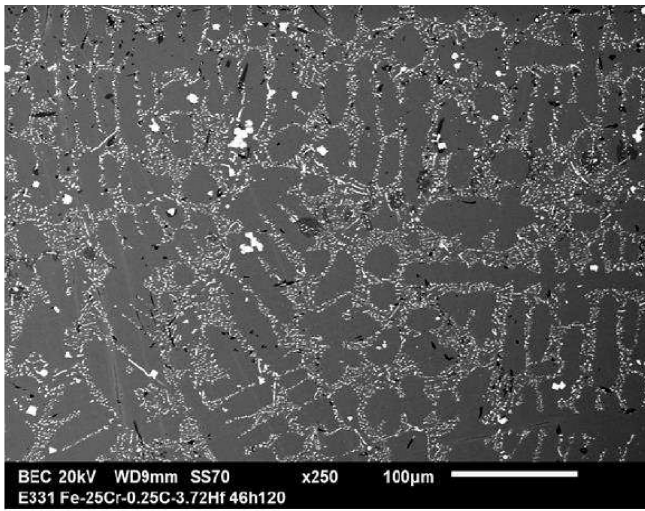


Figure 7 : The bulk's microstructure of the Fe-25Cr-0.25C-3.72Hf alloy after 46 hours at 1200°C (two magnifications and insertion of the initial microstructure in the top-right corner of the second SEM/BSE micrograph)

Figure 8 : The bulk's microstructure of the Fe-25Cr-0.50C-3.72Hf alloy after 46 hours at 1200°C (two magnifications and insertion of the initial microstructure in the top-right corner of the second SEM/BSE micrograph)

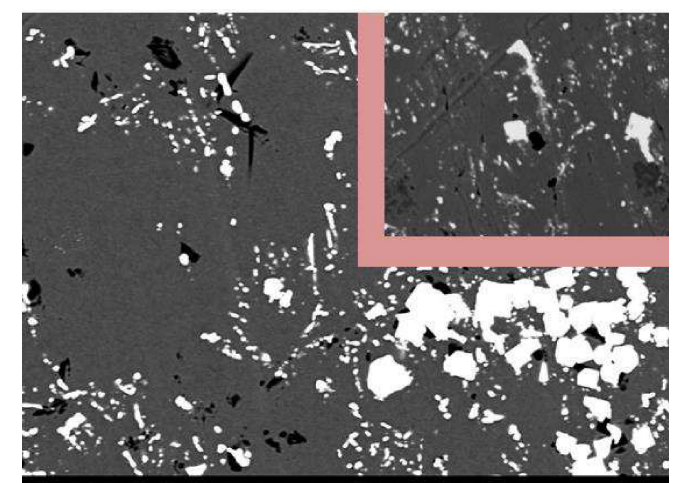
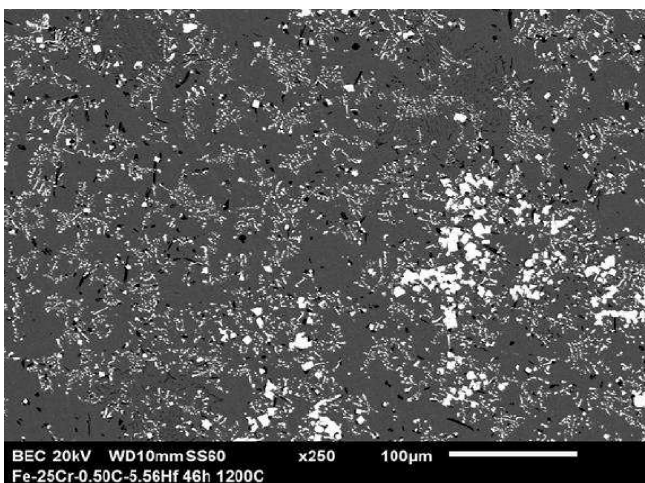


Figure 9 : The bulk's microstructure of the Fe-25Cr-0.50C-5.58Hf alloy after 46 hours at 1200°C (two magnifications and insertion of the initial microstructure in the top-right corner of the second SEM/BSE micrograph)

Full Paper

the HfC carbides really ensure a good strengthening of the alloys and second keep an eye on the consequences of the internal oxidation of these carbides which may be propagated to the core of the alloys.

CONCLUSIONS

The presence of hafnium with so high contents in these alloys thus led to mass gain rates only slightly higher than in absence of hafnium, for Hf contents remaining lower than 4wt.%. The kinetics are similar to the corresponding Hf-containing nickel alloys earlier studied and much slower the very fast ones observed for the corresponding cobalt alloys. This shows that a supplementary protection by increase in bulk chromium content or by surface chromium-enrichment – as envisaged for the latter cobalt alloys – is not necessary, at least to experimentally verify the mechanical strengthening initially expected by promoting the HfC formation. But some indications as the presence of iron oxide and of local thick oxides on surfaces, as well as the internal oxidation observed very deeply for some alloy, let think that catastrophic oxidation may occur not very late at this very high temperature of 1200°C. In case of lack in either oxidation resistance of long times or of not sufficient efficiency of high temperature strengthening, other types of MC carbides, as ZrC^[12], may be considered in the future to replace these HfC carbides.

ACKNOWLEDGMENTS

The authors gratefully thank Sandrine Mathieu for the SEM/EDS analyses and Pascal Villeger for the XRD runs.

REFERENCES

- [1] T.B.Shaffer; High-Temperature Materials- N°1: Materials index, Plenum Press, New York, (1964).
- [2] C.T.Sims, W.J.Hagel; The Superalloys, John Wiley and Sons, New York, (1972).
- [3] E.F.Bradley; Superalloys: A Technical Guide, 1st Edition, ASM International, Metals Park, (1988).
- [4] P.Kofstad; High Temperature Corrosion, Elsevier applied science, London, (1988).
- [5] J.M.Dorlot, J.P.Bailon, J.Masounave; Des matériaux, Editions de l'école polytechnique de Montréal, Montréal, (1986).
- [6] P.Berthod, Y.Hamini, L.Aranda, L.Héricher; Calphad, **31**, 351 (2007).
- [7] P.Berthod, Y.Hamini, L.Héricher, L.Aranda; Calphad, **31**, 361 (2007).
- [8] P.Berthod; Materials Science: An Indian Journal, **9(12)**, 453 (2013).
- [9] E.Conrath, P.Berthod; Materials Science: An Indian Journal, in press.
- [10] E.Conrath, P.Berthod; Materials Science: An Indian Journal, **10(1)**, 30 (2013).
- [11] P.Berthod, E.Conrath; Materials Science: An Indian Journal, **10(1)**, 38 (2013).
- [12] P.Berthod; Journal of Alloys and Compounds, **481**, 746 (2009).